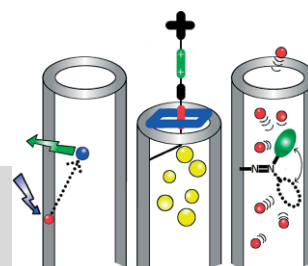


DOI: 10.1002/adfm.200601217

Mesostructured Silica Supports for Functional Materials and Molecular Machines**

By Sarah Angelos, Erik Johansson,
J. Fraser Stoddart,* and Jeffrey I. Zink*



Mesostructured silica thin films and particles prepared by surfactant-templated sol-gel techniques are highly versatile substrates for the formation of functional materials. The ability to deliberately place molecules possessing desired activities in specific spatially separated regions of the nanostructure is an important feature of these materials. Such placement utilizes strategies that exploit the physical and chemical differences between the silica framework and the templated pores. As an example of placement of pairs of molecules, donor and acceptor molecules can be targeted to different regions of mesostructured thin films and energy transfer between them can be measured. The results not only demonstrate the spatial separation but also are used as a molecular ruler to measure the average distance between them. Mesostructured silica is also an excellent support for molecular machines. Molecules that undergo large amplitude motion, when attached to the silica, can function as impellers and nanovalves when activated by light, electrical (redox) and chemical (pH, competitive binding) energy. Derivatized azobenzene molecules, attached to pore walls by using one of the placement strategies, function as impellers that can move other molecules through the pores. Rotaxanes and pseudorotaxanes, placed at pore entrances, function as gatekeepers that can trap and release molecules from the pores when stimulated. Deliberately placed functional molecules on and in mesostructured silica offer many possibilities for both fundamental studies on the nanoscale and for applications in fields as diverse as fluidics, biological drug delivery and controlled release.

1. Introduction

A machine is a device that consists of a solid support with moving parts that carries out a desired function. A machine requires a source of power; light, electrical or chemical energy are the most common. In the case of a molecular machine, the support (or its critical components) must be of the appropriate dimensions (nanometers) in order for the device to function. In addition, the nanostructured supports must be robust and compatible with the power supply. A versatile support that meets these criteria is mesostructured silica made by the sol-gel process.

Synthesis of inorganic oxide materials, especially silica, by sol-gel methods has a long history and has been reviewed extensively.^[1-3] The specific method used by us in this paper involves the hydrolysis and condensation reactions of a tetraalkoxysilane such as tetraethoxysilane (TEOS) with water. After drying, the xerogel is a transparent and stable material containing amorphous pores. The earliest functional sol-gel materials were based on physical immobilization of molecules in the pores. For example, optical sensors based on molecules that produce an optical response caused by the analyte, ranging from simple acid-base indicators to complex biosystems such as enzymes, is still an active area of investigation.^[4-10] Mesostructured silica was first reported in 1992 in the form of surfactant-templated particles.^[11] Both mesostructured particles, and more recently films,^[12-14] have been well studied and an extensive background has developed on the self-assembly of metal oxides based on surfactant and block copolymers as the structure-directing agents.^[3,15-18]

Paralleling the development of the field of mesostructured silica has been the derivatization of the materials with active molecules in order to develop function,^[19] or study film properties.^[20] We recently reported one-step, one-pot synthetic strate-

[*] Prof. J. F. Stoddart, Prof. J. I. Zink, S. Angelos, E. Johansson
Department of Chemistry and Biochemistry and
California Nanosystems Institute
University of California
Los Angeles, CA 90095 (USA)
E-mail: stoddart@chem.ucla.edu; zink@chem.ucla.edu

[**] This work was made possible by grants from the US National Science Foundation (CHE 0507929, DMR 0346601), and FENA. The authors acknowledge the contributions by the many co-workers whose accomplishments are cited in the references.

gies involving materials made by “Evaporation Induced Self Assembly”^[12,21] to place deliberately photoactive molecules in the spatially separated regions of the mesostructure.^[22–25] In this approach, all of the components (including the molecules chosen to develop a specific function and the structure directing agents) are dissolved in the starting sol. Dip coating of this sol onto a substrate produces doped mesostructured films. The earliest examples of placement used luminescent molecules that were designed to probe the film formation.^[26–29] The micelle assembly process was monitored and correlated with changes in solvent composition. Probes that were preferentially incorporated in specific regions (such as the micelle interior) were used. In the most recent examples, designed simultaneous placement of two or more molecules has been demonstrated and detailed studies of spectroscopic properties and energy transfer between molecules have been reported.^[25]

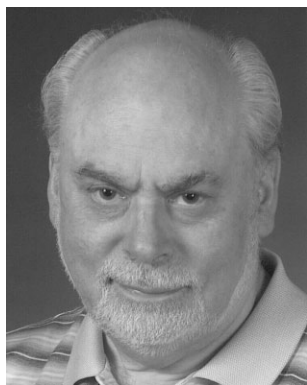
Other structured, pore containing materials including mesostructured titania and zirconia, and microporous zeolites have received considerable attention as well.^[30–34] Meso- and macrostructured titania have been synthesized, and post synthesis treatment used to induce wall crystallinity without cracking.^[30] Mesoporous titania and zirconia, with cubic or 2D hexagonal structure, has been synthesized and further derivatized using post grafting.^[31] Zeolites have been grafted with azobenzene units and the cis/trans isomerization of the azobenzene used to control gas permeability.^[32] Zeolites have also been used as photonic antennas by doping them with luminescent molecules.^[34] Mesoporous silica containing photo electron donors was covered with electron acceptor-containing titania nanosheets for

long lived charge separation.^[33] Considerable advances in functionalizing these materials have also been made using both one pot one step derivatization and derivatization after completion of their synthesis (post synthesis grafting).^[19,31,35–37]

In this feature article, we focus on the uses of mesostructured silica supports for functional materials and molecular machines. We begin with a discussion of strategies for placement of photoactive molecules in specific spatially separated regions of the nanostructure.^[12,21] Energy transfer between pairs of molecules is introduced as an example of an induced optical function, as confirmation of the designed placement, and as a molecular ruler to measure distances in the framework. The major application of the silica structure that we then discuss is molecular machines. Molecules that undergo large amplitude motion, the moving parts, are attached to the framework. Spectroscopic investigations of the motion are discussed, and the useful work in the form of molecular impellers in nanopores powered by light and molecular valves controlling the pore openings powered by chemical, electrical and light energy are described. Mesostructured silica is a very versatile and useful support for many types of functional materials.

2. Designed Placement of Molecules in Mesostructured Silica

Optical or mechanical activities can be achieved in the nanostructured silica by incorporating molecules with the desired functionality in the material. The nanometer size scale of the



J. Fraser Stoddart was born in Edinburgh, Scotland in 1942. He received all (B.Sc., Ph.D., and D.Sc.) of his degrees from the University of Edinburgh, UK. In 1967, he went to Queen's University (Canada) as a National Research Council Postdoctoral Fellow, and then in 1970, to Sheffield University as an Imperial Chemical Industries (ICI) Research Fellow, before joining the academic staff as a lecturer in Chemistry. After spending a sabbatical (1978–1981) at the ICI Corporate Laboratory in Runcorn, he returned to Sheffield where he was promoted to a readership in 1982. In 1990, he took up the Chair of Organic Chemistry at Birmingham University and was Head of the School of Chemistry there (1993–1997) before moving to UCLA as the Saul Winstein Professor of Chemistry in 1997. Presently, he holds the Fred Kavli Chair in NanoSystems Sciences at UCLA and is the Director of the California NanoSystems Institute. His current research interest are concerned with transporting well-established concepts in biology from the life sciences into materials and medicinal chemistry.



Jeffrey I. Zink is a Distinguished Professor of Chemistry in the Department of Chemistry and Biochemistry and a member of the California Nanosystems Institute at the University of California Los Angeles (UCLA). He received his Bachelors of Science degree at the University of Wisconsin and his Ph.D. degree at the University of Illinois Urbana-Champaign under the supervision of Russell S. Drago. After graduation he joined the faculty at UCLA as an assistant professor. His research interests include excited state properties of metal-containing molecules (especially excited state distortions and excited state mixed valence) studied by electronic and resonance Raman spectroscopy and the time-dependent theory of spectroscopy, triboluminescence, sol-gel optical and biomaterials, and nanostructured functional materials. In the latter area, he and his research group are particularly interested in electron and energy transfer and in molecular machines.

materials precludes fabrication by conventional technologies such as machining, etching or photolithography. A synthesis method such as EISA that involves a continuous “bottom up” process is needed where the desired material forms in a single step and both the structural and functional molecules arrange themselves within the developing mesostructure (Fig. 1).

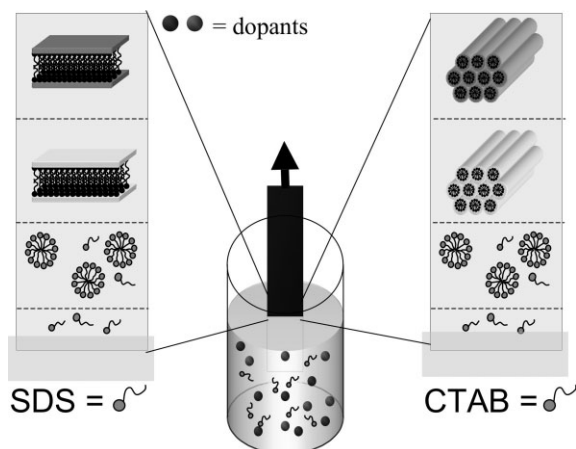


Figure 1. Evaporation induced self assembly during dip coating to form lamellar (left) and 2D hexagonal (right) mesostructures. A glass or silicon substrate is dipped into the solution after which the substrate is retracted, pulling with it a thin film of liquid. Ethanol will evaporate preferentially from the film of liquid, raising the concentration of acid and surfactant. The silica oligomers arrange themselves around the liquid crystal phase and condensation continues yielding the surfactant templated, nanostructured silica thin film as illustrated for sodium dodecylsulfate (SDS) and cetyl trimethyl ammonium bromide (CTAB).

The specific structure that is obtained (a hexagonal array of rods when cetyl trimethyl ammonium bromide, CTAB, is used as the structure directing agent) has chemically and physically different regions in which functional molecules can be placed selectively in a one-pot one-step self assembly process (frequently called co-condensation in the case of particles). Care must be taken because adding a dopant into the sol can have unexpected consequences on the mesostructure. For example, increasing the concentrations of the dopant carbazole causes the structure of a CTAB templated film to change from hexagonal to lamellar.^[38] Alternatively, post-synthesis attachment (frequently called grafting) to attach desired molecules to accessible surfaces can also be used.^[19,31,33,35,36]

2.1. Structural Regions for Separating Donors and Acceptors and Strategies for Placing Active Molecules in Desired Regions

On the molecular level, the structures that are formed have three distinct regions that are important in designing functional materials. The regions are shown in Figure 2.

Our group’s main focus in the past has been to functionalize the mesostructures using a one pot one step method and combinations of three attachment strategies. In this method all dopants are present in the initial sol and the mesoporous film

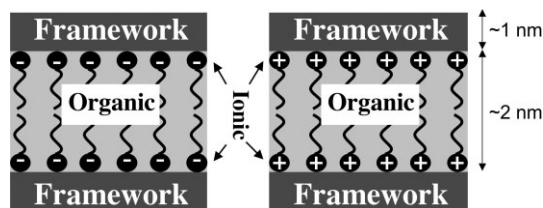


Figure 2. The spatially separated regions of nanostructured sol-gel films templated by ionic surfactants. There are three regions: the silica framework that holds the structure together; the *organic* region containing the hydrophobic long-chain hydrocarbon tails of the surfactant; and the *ionic* region that contains the ionic head group of the surfactant and the counterions. The thickness of the framework depends on sol composition and pulling speed. The dimensions of the organic region are controlled by the length of the hydrocarbon tail of the surfactant used in the preparation. In CTAB templated films, the rod-shaped organic region is about 2 nm in diameter. The ionic region is a few angstroms thick and forms the interface between the framework and the organic region.

that forms is derivatized during the same step as the film formation. Multi-step methods for functionalizing mesostructured silica involve synthesizing the material and then post-synthetically either chemically attaching molecules, or simply filling the pores.^[31,35,36,38] All of these strategies and methods are discussed in this section.

2.1.1. Philicity Strategy: Placement Based on Solubility Differences

The segregation of molecules into chemically different regions of a sol-gel mesostructure is accomplished easily by exploiting the ‘philicity’ or local solubility of the dopant molecules. Hydrophobic molecules will reside in the organic region of the final material, and ionic molecules in the ionic region. The functional molecules are included in the initial sol, and co-assemble into their favored regions during the evaporation induced self-assembly process. The most common examples of this strategy involve hydrophobic molecules; these molecules are incorporated inside the micelles among the hydrocarbon tails, and in the final structure they will reside in the organic region. Proof of the utility of this simple method is provided by our prior work with pyrene that we used as a probe of micelle formation,^[26,27] and R6G that we used as an energy acceptor as discussed below. Furthermore, this method has been used to make titania waveguides,^[39] and fluorescent silica/polymer nanocomposites.^[40]

2.1.2. Bonding Strategy: Donors and Acceptors as Framework Structural Materials

The method of choice for deliberately placing the donor or acceptor in the framework region of the material is to make the active molecule the building block of the framework. In this method, the active molecule itself will form part of the framework.^[22–25] The strength of this method is that the active molecules will be precisely located in the final self-assembled material because it is a fundamental part of the inorganic framework of the material. The major requirements are that

the molecule must itself undergo hydrolysis and condensation in order to form the framework and it also must allow templating by the micelles to occur before the final framework is formed. Examples of ligands that we used to place photoactive and electroactive metal complexes in the framework are shown in Figure 3. Another example of the bonding strategy is to build the framework exclusively from the functional molecule. Recently reported is the successful synthesis of mesostructured

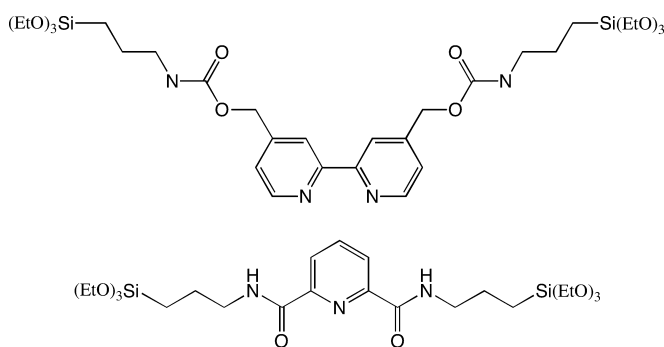


Figure 3. Examples of ligands that place photoactive and electroactive metal complexes in the framework. The ligands above coordinate to metals and the alkoxy silane arms direct the placement in the framework.

materials with both lamellar and 2D-hexagonal periodicity on the mesoscale, where the framework consists of phenyl or biphenyl silsesquioxanes that themselves are stacked in a lamellar fashion, thus providing order on the sub nanometer scale in the framework.^[41–43] These materials, with their high degree of order, open up numerous possibilities for constructing new structures and functions.^[43]

2.1.3. Bifunctional Strategy—Chemical Bonding at the Framework-Ionic Interface

An active molecule can be placed at the interface between the framework and the ionic region by chemically bonding it to the outside of the framework. This method can be achieved, for example, by making one end of the molecule a trialkoxysilane and the other end hydrophobic.^[22–25,35] An example of a molecule that we attached by this strategy is shown in Figure 4. It undergoes large amplitude motion upon absorption of a photon and can function as a molecular machine.^[44] The bifunctional method offers great versatility. It is relatively easy to derivatize a donor or acceptor molecule with a trialkoxy silane using well-established procedures.^[35] The length of the chain between the silicon and the donor or acceptor will determine the distance between the framework wall and the active part of the molecule.

Another method that can be used is to make the functional molecule part of the templating agent, that is, make it a surfactant. Luminescent surfactants have been made and employed successfully to make mesostructured materials.^[45] Another example of functional surfactants is the well-known electron acceptor methyl viologen, derivatized with a long hydrocarbon

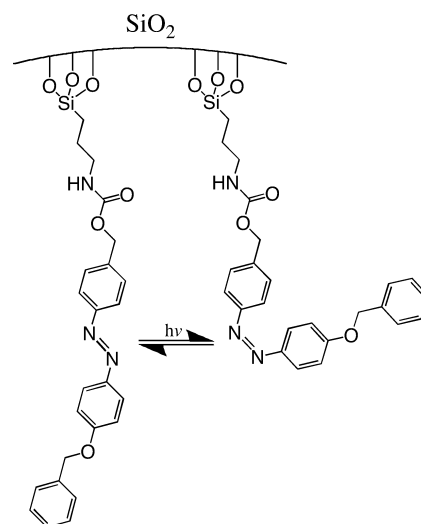


Figure 4. Azobenzene derivative tethered to the silica pore wall via the bifunctional placement strategy. The molecule is covalently linked to the silica pore wall while the hydrophobic nature of the rest of the molecule places that part in the organic region.

tail. Asymmetrical viologens having a long hydrocarbon tail have been extensively studied when incorporated into micelles.^[46–48] It is clear that they retain their function as reversible electron acceptors making them feasible components for molecular power supplies.

2.1.4. Post Synthesis Grafting Strategy

There are cases when it is advantageous to use a multi step process: production of the mesoporous film followed by its derivatization. An important advantage is that the film can be derivatized with species incompatible with the chemistry of the initial sol but a disadvantage is that only accessible surfaces can be derivatized. Post-synthesis grafting involves the same types of alkoxy silane or chlorosilane linkers that are commonly utilized in the bifunctional strategy. A wide variety of functionalized materials have been produced using the post synthesis grafting method,^[19,35] specific examples include mesostructured selective titania membranes,^[36] bifunctional accessible mesopores,^[31] hybrid materials for light induced charge separation^[33] and zeolites with coumarins for light harvesting.^[49] The organic functionality that is introduced to the material can also act as a site for further derivatizations. For example, we used alkoxy silane linkers tethered to surface of mesoporous silicates post-synthetically to position rotaxanes and pseudorotaxanes that function as nanovalves.^[37,50–53]

2.1.5. Backfilling Strategy

Backfilling is a simple strategy for introducing active molecules into the empty pores of mesostructured silica. Empty mesopores are loaded with active molecules by exposing a material to either a solution or vapor containing the active molecules. While this strategy is not a means of chemically modifying po-

rous materials, it is widely useful. Backfilling from either the solution or gas phase is a common method for loading active guests into zeolitic materials.^[32,54,55] Using a combination of backfilling and photoexcitation, the ability of zeolites to selectively incorporate molecules of a certain size but exclude those larger has been used to isolate pure samples of molecules that otherwise exist in a cis/trans equilibrium.^[56] In mesoporous silicate materials, there are cases in which non-covalent modification is desirable. For example, the ability to load luminescent guest molecules into empty mesopores of mesostructured silicates via backfilling is an important step in the study of nanovalves, as will be discussed later.

3. Energy Transfer

A good example of functionality induced in nanostructured films is energy transfer between spatially separated donor and acceptor molecules.^[25] We used quantitative measurements of energy transfer, in conjunction with spectroscopic wavelength shifts, to demonstrate that spatial separation on the nano-scale actually does occur. In addition, energy transfer was used as a molecular ruler to study material properties. Energy transfer and electron transfer, in materials other than mesoporous silica, are also much studied areas. Various donor and acceptor molecules have been incorporated into the channels of zeolitic materials in order to build artificial photonic antenna systems.^[34] The unique properties of zeolites have been studied and taken advantage of in order to generate charge separated pairs.^[57,58]

The silicate thin films that were used by us in the energy transfer studies had a 2D hexagonal structure templated by CTAB. The films were doped simultaneously with two different luminescent molecules, rhodamine 6G (R6G) and a Tb complex (Fig. 5).^[25]

Luminescence spectroscopy showed that R6G, the molecule chosen as the energy acceptor, was incorporated in the surfactant micelles and that the Tb complex chelated by an alkoxy-silylated ligand was incorporated in the silicate framework. Steady-state luminescence spectra, lifetime measurements of R6G luminescence and lifetime measurements on the Tb complex's emission provided evidence of energy transfer. The Tb luminescence lifetime measurements were used to calculate the distance between Tb and R6G in nanostructured films according to the Förster model.

3.1. Luminescence Spectra and Lifetimes

Luminescence spectra and luminescence lifetimes of R6G verified that energy transfer from Tb to R6G occurs. Luminescence spectra excited at the absorption maximum of the Tb li-

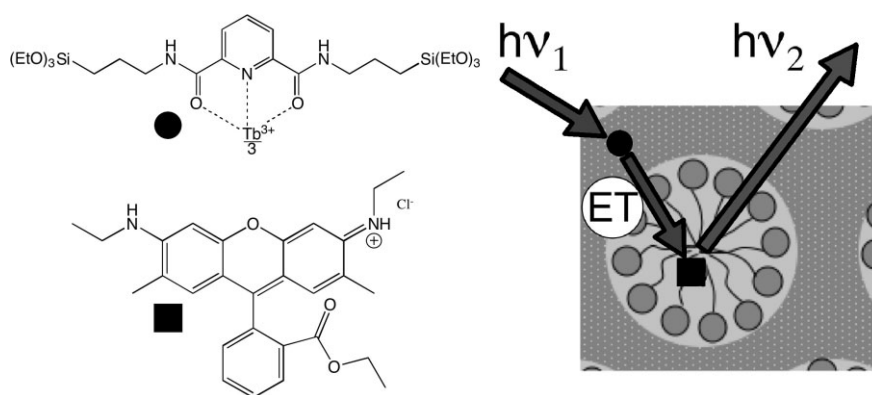


Figure 5. Terbium complex (left top) and Rhodamine 6G (left bottom). Energy transfer takes place from the photoexcited terbium complex in the framework to Rhodamine 6G in the micelle (right).

gand showed enhanced, or sensitized, R6G emission in films with Tb relative to the emission of films without Tb.

In a complementary experiment, the photoexcitation spectra for R6G showed a new peak in the ultraviolet region when the Tb complex was present. The position of the new peak corresponded exactly to the Tb complex's photoexcitation maximum. The appearance of this peak in the photoexcitation spectra of R6G proved that energy transfer occurred because it clearly established the dependence of R6G fluorescence on the Tb complex's absorbance.

Fluorescence lifetime measurements carried out on R6G showed that its lifetime increased as much as three orders of magnitude (to 1.55 microseconds) as the concentration of the Tb complex increased. The complementary effects were observed in the Tb luminescence lifetimes: when the R6G concentration was high, the Tb lifetime was short, and vice versa.

3.2. Distance between Tb and R6G

The donor and acceptor are separated in space in the different regions of the nanostructured thin films: R6G in the micelles and the Tb complex in the silicate framework. In order to use the Förster model to calculate the separation between the two, the Förster radius must be on the same order as the distance from the center of the hydrophobic region inside the micelles to the center of the silicate framework. This distance is about 20 Å, one-half of the *d*-spacing calculated from the XRD pattern. The calculated Förster radius R_0 of 40 Å makes the Tb-R6G system suitable for this analysis.

The efficiency of energy transfer, E , was calculated by using Equation 1.

$$E = \frac{R_0^6}{R^6 + R_0^6} = 1 - \frac{\tau_{DA}}{\tau_D} = 1 - \frac{F_{DA}}{F_D} \quad (1)$$

where E is the calculated quenching efficiency, t_D and F_D are the lifetime and fluorescence intensity of the donor in the absence of acceptor, and t_{DA} and F_{DA} are the corresponding quantities in the presence of acceptor.^[59] The Förster radius and the experimentally obtained quenching efficiencies

were used to solve Equation 1 for R , the donor-acceptor distance.

The average Tb-R6G distance decreased as R6G concentration was increased. At the lowest R6G to Tb concentration ratio studied, R6G:Tb 1.6:100, a small quenching of 5% was measured, corresponding to a large average Tb-R6G distance of $R = 65 \text{ \AA}$. This distance decreased as R6G concentration increased until it reached a minimum value of 29 \AA at R6G:Tb 20:100.

This study demonstrated that self-assembly resulted in spatially separated donor and acceptor molecules in transparent nano-structured optically transparent continuous thin films. More detailed analyses of the energy transfer and spectra are discussed in the paper. The preparation strategies for separating active molecules are simple and expandable to a wide variety of donor and acceptor molecules for both photo-induced energy transfer and electron transfer.

4. Silicate Films and Particles as Supports for Molecular Machines

In this section, we will describe the design and synthesis of hybrid materials consisting of mesostructured silicate supports and switchable organic molecules.^[32,34,60–64] Two types of molecular machines will be discussed: photoresponsive impellers based on azobenzene derivatives, and supramolecular nanovalves based on [2]rotaxanes and [2]pseudorotaxanes. The silicate supports used include 2D hexagonal thin films, and also mesoporous nanoparticles. Thin films offer the advantage of convenient handling because they are attached to macroscopic substrates, while particles have more surface area and also better defined pore openings.

4.1. Azobenzene as a Nano-Impeller

Photo-responsive materials functionalized with azobenzene have been developed in a range of inorganic hosts, and a variety of applications are envisioned for these materials. Meso-structured silica thin films with azobenzene derivatives bridged within the framework have been synthesized, and the ability to photoresponsively change the d-spacing of these materials has been demonstrated.^[60,61] The bridging azobenzenes were attached by derivatizing both ends of the molecule with ethoxysilanes, and co-condensing them into the mesostructure during the evaporation induced self-assembly process. Functional silicate materials have also been synthesized by tethering one end of an azobenzene derivative to the pores walls of an cubic-structured nanoporous membrane such the effective pore size could be optically controlled, ultimately affecting the rate of mass transport through the membrane.^[62] The development of photoresponsive, azobenzene-functionalized materials has not been limited to silicates. For example, zeolitic materials containing adsorbed azobenzene molecules have been prepared, and the photoswitchable permeation of these membranes has been demonstrated as a result of the azobenzene cis–trans photoisomerization.^[32]

4.1.1. Photophysical Studies of Azobenzene Motion in Mesopores

We reported detailed photophysical studies of a series of azobenzene derivatives in mesostructured silicate thin films and particles.^[44] One end of the azo molecules was derivatized so it can be attached to silica while the other end was derivatized with generation zero to generation three of the *Fréchet* dendron. The size and weight increase from generation zero to three. Azobenzene-functionalized thin films were prepared by first coupling the azo molecule to an isocyanatotriethoxysilane linker (ICPES) and then adding this compound to the sol. During film pulling, the ethoxysilane moieties condense into the silica framework with the result that the azobenzene machines are covalently tethered to the pore walls (bifunctional strategy, Fig. 4). After template removal by solvent extraction, fluorescence spectroscopy was used to confirm that the trans-cis isomerization of azobenzene occurs reversibly in the nanopores. Photophysical properties of the azo derivatives in mesostructured particles prepared by a base catalyzed sol–gel method was also studied. The pores were templated by cetyltrimethylammonium bromide (CTAB) surfactants, and empty pores were obtained by template removal using solvent extraction.

The thermal cis to trans isomerization rate constant in solution is similar for all generations of azo molecules ($k = 3.3 \times 10^{-6} \text{ s}^{-1}$ for generation zero to $k = 2.6 \times 10^{-6} \text{ s}^{-1}$ for generation three) and can be understood as the small terminus of the molecule moving because it is almost the same for all of these azo molecules. The properties of the molecules covalently attached to the pore wall of MCM-41 particles and 2D hexagonal silica films were different. Large changes in the rate constants for the thermal cis to trans isomerization of the azo derivatives were observed in the series of small ($k = 1.02 \times 10^{-5} \text{ s}^{-1}$) to the large molecule ($k = 2.6 \times 10^{-6} \text{ s}^{-1}$). These changes imply that the dendrimer is moving and there is a clear dendritic effect. Luminescence spectra were also used to monitor the switching. With excitation at 351 nm, structured emission centered at 450 nm was observed and assigned to the cis isomer. With excitation at 457 nm, $n\pi^*$ -emission from the trans isomer was observed at 550 nm.

4.1.2. Azobenzene as a Molecular Impeller

The photophysical studies suggested that the motion could be used as an “impeller” when the azobenzene is excited at 450 nm.^[44] The trans to cis isomerization quantum yield at 450 nm is 0.36 and that for cis to trans is 0.64. Continuous excitation at this wavelength produces constant isomerization reactions and results in continual dynamic wagging of the untethered terminus. We showed that when the pores are loaded with luminescent probe molecules and the azobenzene motion is stimulated by light, photoinduced expulsion of the probe from the particles caused by the motion could occur (Fig. 6).^[65]

We demonstrated successful use of the azobenzene motion as an impeller by attaching the small AzoH onto the pore interiors. Real time measurements of the rate of expulsion of two different dyes, Coumarin 540A and Rhodamine 6G were made by using luminescence spectroscopy. The pores were loaded

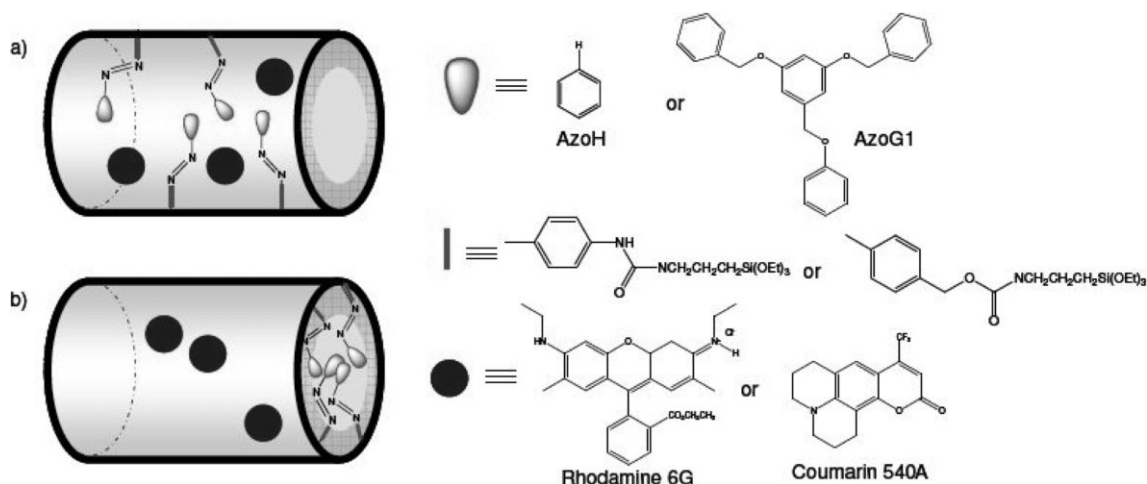


Figure 6. Photoisomerization of azobenzene derivatives a) inside of a nanopore and b) at the entrance of a nanopore.

with dye molecules by soaking the particles in 1 mM solutions of the dye overnight and then washing to remove adsorbed molecules from the surface. Dye-loaded particles (~15 mg) were placed in the bottom of a cuvette and 12 mL of MeOH was carefully added. A 1 mW probe beam directed into the liquid was used to excite dissolved dye molecules that are released from the particles (540 nm for Coumarin 540 A and 562 nm for Rhodamine 6G; Fig. 7).

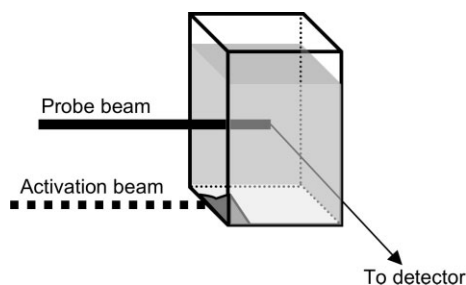


Figure 7. Experimental geometry for measuring expulsion of molecules from pores. The activation beam excites the particles; the probe beam excites the probe molecules released into solution.

The spectrum excited by the probe beam was recorded as a function of time at 1-s intervals. After 5 minutes, a 9 mW excitation beam was used to directly irradiate the functionalized particles and excite the azobenzenes' motions. Plots of the dissolved dye intensity as a function of time (the release profiles) indicate that the particles hold the guest molecules but expel them when stimulated (Fig. 8).

As a control experiment to verify that azobenzene excitation drives the release, the particles were irradiated with equal power at a wavelength (647 nm) at which the azobenzene does not absorb. The red light had no effect on the release. These results demonstrated that the system only responds to wavelengths that drive the large amplitude azobenzene motion.

The expulsion of molecules from pores containing azobenzene molecules attached internally probably involves an "im-

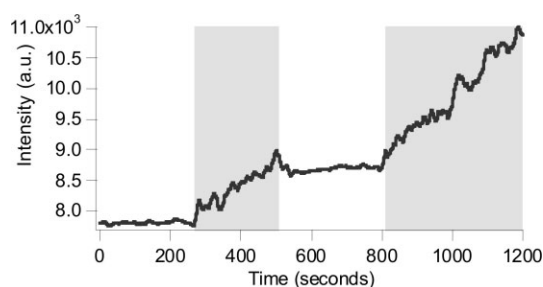


Figure 8. Time dependence of the expulsion of coumarin probe molecules. No expulsion occurs when the activation light is off. The coumarin expelled into solution increases when the activating light is on.

pellor" mechanism. Prior to excitation, dye molecules are held inside the particles because the pores are considerably congested by the static azobenzene machines and a facile pathway for escape is not available. Excitation of the azobenzenes causes them to wag back and forth, effectively imparting motion to the trapped dye molecules and allowing them to traverse the pore interior until they escape. These results open the possibilities of trapping useful molecules such as drugs and releasing them on demand.

4.2. A Reversible Nanovalve

Various approaches, in addition to isomerization of azobenzenes, for controlling the release of molecules trapped in the pores of functionalized mesostructured silica nanoparticles have been investigated. For example, the photoactivated intermolecular dimerization of tethered coumarins has been shown to successfully regulate access to the mesopores of MCM-41, such that guest molecules are controllably trapped and released from the host nanoparticles.^[63] In addition, chemically removable CdS nanoparticles are able to cap the mesopores of MCM-41 type materials, effectively encapsulating guest molecules by blocking pore entrances and allowing them to escape upon removal of CdS caps.^[64]

We have reported nanovalves based on supramolecular motifs that use mesoporous silica as their solid support.^[37,50–53,66] The moving part consists of a ring (cyclic molecule) that slides on a thread-like molecule between one or more binding stations (Fig. 9).

The thread is attached at or in the opening to a pore. The movable ring acts as a gatekeeper; when it is positioned at the pore opening it blocks other molecules from entering or escaping from the interior of the pore, but when it moves to a position more distant from the pore opening the molecules can move in or out of the pore.

We have developed and investigated different types of supramolecular nanovalves, each relying on a distinct motif for complexation between the ring and thread components. Ultimately, the components selected and the interactions occurring between them determine the type of stimulus that is required for valve activation. One type of ring component that has been utilized in the design of redox-active nanovalves is cyclobis(paraquat-*p*-phenylene) (CBPQT⁴⁺). The tetracationic cyclophane complexes with a tetrathiafulvalene (TTF) station electrostatically, but can be repelled away from the station upon a 2 electron oxidation of the TTF. Another nanovalve design uses dibenzo[24]crown-8 (DB24C8) rings as the movable components, which complex with dialkylammonium threads. Hydrogen bonding interactions between the ring and thread hold this nanovalve in the closed configuration. The interactions can be interrupted, thereby causing the valve to open, by introduction of a base to deprotonate the thread, or by metal cations which can competitively bind the DB24C8 rings.

The properties of the nanovalves are investigated by opening the valves, filling the pores by allowing desired molecules to diffuse into the empty pores, closing the valves to trap the molecules, and measuring the release of the molecules when the pores are again opened (Fig. 9). The release of luminescent probe molecules into solution is monitored over time using luminescence spectroscopy. The nanoparticles are luminescent

when the probes are trapped in them, and the luminescence of the solution increases as the probe molecules are released.

The functional material was placed at the bottom of a solvent filled quartz cell and only the liquid above the solid powder was exposed to the probe light beam. The increase in the luminescence intensity as a function of time will measure the rate of escape of the probe. If the valve leaks, an increase will be observed before the valves are activated.

4.3. Methods of Activating Supramolecular Nanovalves

4.3.1. Activation by Oxidizing the Thread

A nanovalve capable of reversibly trapping and releasing guest molecules from the pores of MCM-41 has been demonstrated.^[50] The actuating component in this system was a redox-controllable [2]rotaxane consisting of a thread with two recognition stations and a movable CBPQT⁴⁺ ring. A TTF station was positioned furthest from the silica support, and the CBPQT⁴⁺ ring thermodynamically preferred to reside on that station. With the ring encircling the TTF station, the pores were unobstructed and the nanovalve was in its open configuration. Oxidation of the TTF station to give TTF²⁺ destabilized its interaction with the CBPQT⁴⁺ causing the ring to shuttle to the dioxynaphthalene (DNP) station and thus closing the valve. The valve was reopened upon reduction of the tetrathiafulvalene (TTF) station, which caused the ring to shuttle back to the more distant location and unblock the nanopores. Operation of the moving part was monitored by the luminescence of naphthalene. In the closed configuration, the CBPQT⁴⁺ quenched the naphthalene luminescence, and upon activation of the valve an increase in naphthalene emission intensity was observed.

4.3.2. Activation by Reducing the Ring^[37,67]

[2]pseudorotaxanes consisting of 1,5-bis[2-(2-hydroxyethoxy)bisethoxy]naphthalene (BHEEEN) threads encircled by cyclobis(paraquat-*p*-phenylene) (CBPQT⁴⁺) rings were mounted onto the surface that was functionalized with ICPEs. The valve was opened by reduction of the (CBPQT⁴⁺) rings by cyanoborohydride. Emission from the BHEEEN was monitored and used as an indicator of the threading-dethreading process of the machines.

4.3.3. Activation by Light

The [2]pseudorotaxane system discussed above was reconfigured for light activation. Molecules that become strong reducing agents in their excited electronic states such as anthracene carboxylic acid and trisbipyridine ruthenium(II) were attached to the silica. Photo-induced electron transfer from the sensitizer to the CBPQT⁴⁺ rings opened the valves (Fig. 10).

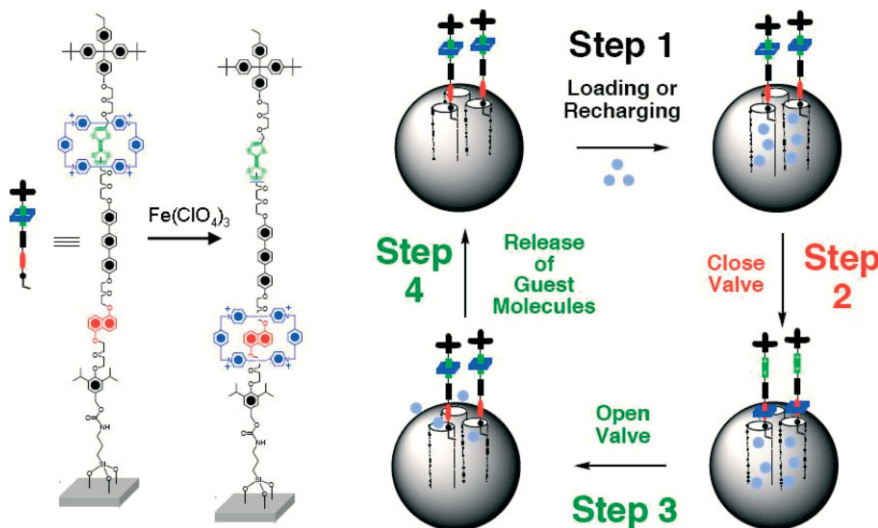


Figure 9. A reversible molecular valve. Copyright 2005, National Academy of Sciences: reproduced with permission from reference [49].

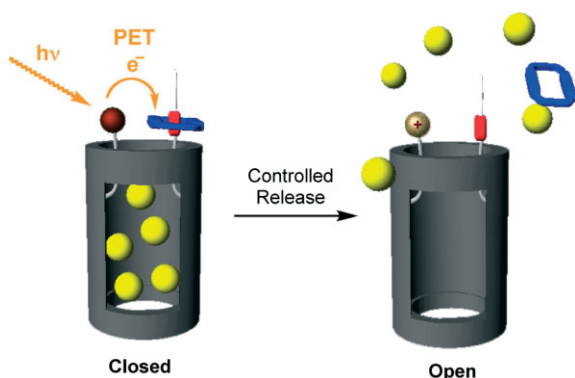


Figure 10. Light-controlled nanovalve operation.

4.3.4. Activation by pH^[51]

Pseudorotaxanes based on dialkylammonium threads encircled by dibenzo[24]crown-8 (DB24C8) rings were tethered to an MCM-41 surface to yield pH-driven supramolecular nanovalves.^[51] This system relied on hydrogen bonding for complexation, therefore the components could be made to dissociate upon deprotonation of the threads induced by addition of base. Activation was demonstrated using a variety of bases; the steric size of the activating bases greatly affected the rate of release.

4.3.5. Activation by Competitive Binding^[52]

Competitive binding of metal and fluorodialkylammonium cations has been used as an alternative activation method for nanovalves based on the same DB24C8/dialkylammonium pseudorotaxanes.^[52] Introduction of a species capable of complexation with the DB24C8 rings provided a mechanism of nanovalve activation by shifting the equilibrium of the complexation–decomplexation process of the rings and threads, trapping the rings and preventing them from recomplexing with the threads. The binding affinity of the activating cations toward the DB24C8 rings was the major factor affecting the rate of release.

4.4. Optimization of Molecular Nanovalves

Each step involved in the design of nanovalves affords several options that must be carefully selected to ensure optimal operation of the machines. While the design of the machine itself ultimately determines the mode of activation that will be employed, the techniques for immobilizing the machines onto surfaces play a significant role in the overall performance of the nanovalve. Typically, machines are tethered to the silica surface through the use of silane linkers, which are bifunctional coupling agents with one end able to condense with the silica and the other able to react with the machines.^[53] Some of the critical factors affecting nanovalve operation that we studied include the positioning of the silane linker relative to the pore orifices, the length of the silane linker, the diameters of the pores,

and the size of the trapped molecules. Optimization of the valve requires testing different pore diameters, adjusting the distance of the moving part from the pore opening, adjusting the size of the moving part, and testing activation mechanisms, i.e., “systems engineering”.^[53] In order to optimize the structure–property relationships, the effects of constructing nanovalves using silane linkers with different lengths positioned in different regions relative to the silicate pores’ orifices on the effective release of large and small probe molecules was investigated.^[53] Two linkers of different length, isocyanatopropyltriethoxysilane and chloromethyltriethoxysilane were studied. Two methods of removing the surfactant from the silica pores, calcination and solvent extraction, were used. Synthetic methods that position the linkers in two different locations relative to the pores’ orifices were used: “OUT” where the bonding to the silica is outside of the pores, and “IN” where the bonding is in the interiors of the pores (Fig. 11).

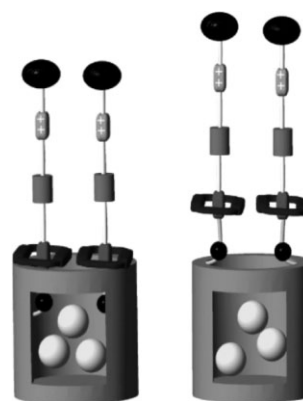


Figure 11. Nanovalves in the IN (left) and OUT locations.

To achieve the OUT location, the linkers were reacted with the silica while the pores are still filled with surfactant, and then the surfactant was removed by solvent extraction. To attach the linkers IN the pores, the surfactant was removed by calcination or solvent extraction such that the small linker molecule can enter the pores and bind in the interiors. The IN configuration can also be achieved by the one-step co-condensation method.

A systematic study was conducted to determine which combination of these factors resulted in optimal machine function. The reversible moving part consisting of bistable [2]rotaxane with a CBPQT⁴⁺ ring and a thread containing DNP and TTF stations was used. When a small probe molecule such as Coumarin 440 was used, valves constructed with moving parts attached with the longest linker, ICPEs, with the IN configuration were leaky. The same valves did not leak when a larger probe molecule such as Rhodamine B was used. The leakage problem was solved by using a much shorter linker, chloromethyltriethoxysilane, that positioned the ring closer to the pore orifice. The maximum occupancy of the payload molecule in the pores occurred when no linkers were attached to the in-

ner pore walls. Attachment of the moving parts with a short linker in the OUT configuration resulted in leak-free valves and was the optimal valve tested.

5. Summary

Nanostructured silica films and particles are versatile frameworks for molecular machines. Their useful properties include ease of synthesis, chemical stability, optical transparency, choice of nanostructure and morphology, and simplicity of derivatization. Active molecules are placed deliberately in specific spatially separated regions in a one-step, one pot synthesis. Energy transfer between donor and acceptor molecules was used to verify their deliberate placement and spatial separation. Molecules that undergo large amplitude molecular motions can function as moving parts and can be chemically bonded in and on the silica. The oscillatory motion of azobenzenes impels molecules through pores and out of nanoparticles. Pseudorotaxanes and rotaxanes open and close pore openings, functioning as valves driven by oxidation and reduction reactions, light, bases and ions. The functional materials described here offer many possibilities for both fundamental studies on the nanoscale and for applications. Messtructured films offer the advantage of ease of handling. The 100 nm thick films (that contain ordered arrays of tubes, sheets, and other structures) are supported on macroscopic substrates that are easy to manipulate and handle. Messtructured particles (nanospheres) are most useful in studies that require nano-containers that are transportable in a broad range of length scales.

The films are most useful when macroscopic manipulation is possible, such as for sensor applications. In addition, they are also well suited for studies of photophysical phenomena (such as energy transfer discussed in this review) or electron transfer (with possible applications in charge separation and energy storage). Studies of fluidics on the nanoscale are also possible in films. Particles have already proven useful as drug delivery systems, and it is likely that increasing effort will be devoted to derivatizing valve particles for active control of drug release in biosystems.

Challenges facing applications of these types of materials are not always obvious. For example, when attempting to use particles as transport containers, especially for biological applications, it is important that they do not agglomerate or aggregate and lose their individual identities. Derivatization of the exteriors may be required. As another example, for biological applications the materials must function in aqueous environments. None of the valves discussed in this review do so; the polarity and hydrogen bonding ability of water inhibit the site recognition motifs that are the basis for the large amplitude motions. A new generation of valves will need to be developed. Likewise new modes of activation will be required; the light-driven impeller does function in water, but it may not always be possible to deliver light to the region where the activation of the impeller is required (such as internal organs of an animal). We expect that innovative and exciting ideas and new applications, none of which have yet been thought about, will appear in the

future. The ease of preparing and derivatizing silica make it a very useful framework for developing new functions and new machines.

Received: December 18, 2006

Revised: April 3, 2007

Published online: August 9, 2007

- [1] C. J. Brinker, G. W. Scherer, *Sol-Gel Science: The Physics and Chemistry of Sol-Gel Processing*, Academic, San Diego, CA **1990**, p. 92 101.
- [2] D. A. Loy, K. J. Shea, *Chem. Rev.* **1995**, *95*, 1431.
- [3] G. J. D. Soler-Illia, C. Sanchez, B. Lebeau, J. Patarin, *Chem. Rev.* **2002**, *102*, 4093.
- [4] L. M. Ellerby, C. R. Nishida, F. Nishida, S. A. Yamanaka, B. Dunn, J. S. Valentine, J. I. Zink, *Science* **1992**, *255*, 1113.
- [5] B. C. Dave, B. Dunn, J. S. Valentine, J. I. Zink, *Anal. Chem.* **1994**, *66*, A1120.
- [6] J. M. Miller, B. Dunn, J. S. Valentine, J. I. Zink, *J. Non-Cryst. Solids* **1996**, *202*, 279.
- [7] B. Dunn, J. M. Miller, B. C. Dave, J. S. Valentine, J. I. Zink, *Acta Mater.* **1998**, *46*, 737.
- [8] D. Avnir, S. Braun, O. Lev, M. Ottolenghi, *Chem. Mater.* **1994**, *6*, 1605.
- [9] D. Avnir, *Acc. Chem. Res.* **1995**, *28*, 328.
- [10] S. Y. Chia, J. Urano, F. Tamanoi, B. Dunn, J. I. Zink, *J. Am. Chem. Soc.* **2000**, *122*, 6488.
- [11] C. T. Kresge, M. E. Leonowicz, W. J. Roth, J. C. Vartuli, J. S. Beck, *Nature* **1992**, *359*, 710.
- [12] Y. F. Lu, R. Ganguli, C. A. Drewien, M. T. Anderson, C. J. Brinker, W. L. Gong, Y. X. Guo, H. Soyez, B. Dunn, M. H. Huang, J. I. Zink, *Nature* **1997**, *389*, 364.
- [13] D. Zhao, P. Yang, N. Melosh, J. Feng, B. F. Chmelka, G. D. Stucky, *Adv. Mater.* **1998**, *10*, 1380.
- [14] P. C. A. Alberius, K. L. Frindell, R. C. Hayward, E. J. Kramer, G. D. Stucky, B. F. Chmelka, *Chem. Mater.* **2002**, *14*, 3284.
- [15] Q. S. Huo, D. I. Margolese, U. Ciesla, D. G. Demuth, P. Y. Feng, T. E. Gier, P. Sieger, A. Firouzi, B. F. Chmelka, F. Schuth, G. D. Stucky, *Chem. Mater.* **1994**, *6*, 1176.
- [16] D. Y. Zhao, P. D. Yang, Q. S. Huo, B. F. Chmelka, G. D. Stucky, *Curr. Opin. Solid State Mater. Sci.* **1998**, *3*, 111.
- [17] M. H. Bartl, S. W. Boettcher, K. L. Frindell, G. D. Stucky, *Acc. Chem. Res.* **2005**, *38*, 263.
- [18] Q. S. Huo, D. I. Margolese, U. Ciesla, P. Y. Feng, T. E. Gier, P. Sieger, R. Leon, P. M. Petroff, F. Schuth, G. D. Stucky, *Nature* **1994**, *368*, 317.
- [19] G. Soler-Illia, P. Innocenzi, *Chem. Eur. J.* **2006**, *12*, 4478.
- [20] T. Keeling-Tucker, J. D. Brennan, *Chem. Mater.* **2001**, *13*, 3331.
- [21] D. Grosso, F. Cagnol, G. Soler-Illia, E. L. Crepaldi, H. Amenitsch, A. Brunet-Bruneau, A. Bourgeois, C. Sanchez, *Adv. Funct. Mater.* **2004**, *14*, 309.
- [22] R. Hernandez, A. C. Franville, P. Minoofar, B. Dunn, J. I. Zink, *J. Am. Chem. Soc.* **2001**, *123*, 1248.
- [23] P. N. Minoofar, R. Hernandez, S. Chia, B. Dunn, J. I. Zink, A. C. Franville, *J. Am. Chem. Soc.* **2002**, *124*, 14 388.
- [24] P. Minoofar, R. Hernandez, A. C. Franville, S. Y. Chia, B. Dunn, J. I. Zink, *J. Sol-Gel Sci. Technol.* **2003**, *26*, 571.
- [25] P. N. Minoofar, B. S. Dunn, J. I. Zink, *J. Am. Chem. Soc.* **2005**, *127*, 2656.
- [26] M. H. Huang, B. S. Dunn, H. Soyez, J. I. Zink, *Langmuir* **1998**, *14*, 7331.
- [27] M. H. Huang, B. S. Dunn, J. I. Zink, *J. Am. Chem. Soc.* **2000**, *122*, 3739.
- [28] M. H. Huang, H. M. Soyez, B. S. Dunn, J. I. Zink, *Chem. Mater.* **2000**, *12*, 231.
- [29] A. C. Franville, B. Dunn, J. I. Zink, *J. Phys. Chem. B* **2001**, *105*, 10335.
- [30] M. C. Fuertes, G. Soler-Illia, *Chem. Mater.* **2006**, *18*, 2109.
- [31] P. C. Angelome, G. Soler-Illia, *J. Mater. Chem.* **2005**, *15*, 3903.

- [32] K. Weh, M. Noack, K. Hoffmann, K. P. Schroder, J. Caro, *Microporous Mesoporous Mater.* **2002**, *54*, 15.
- [33] T. Yui, T. Tsuchino, T. Itoh, M. Ogawa, Y. Fukushima, K. Takagi, *Langmuir* **2005**, *21*, 2644.
- [34] C. Minkowski, R. Pansu, M. Takano, G. Calzaferri, *Adv. Funct. Mater.* **2006**, *16*, 273.
- [35] L. Nicole, C. Boissiere, D. Grosso, A. Quach, C. Sanchez, *J. Mater. Chem.* **2005**, *15*, 3598.
- [36] E. H. Otal, P. C. Angelome, S. A. Bilmes, G. Soler-Illia, *Adv. Mater.* **2006**, *18*, 934.
- [37] R. Hernandez, H. R. Tseng, J. W. Wong, J. F. Stoddart, J. I. Zink, *J. Am. Chem. Soc.* **2004**, *126*, 3370.
- [38] M. H. Huang, F. Kartono, B. Dunn, J. I. Zink, *Chem. Mater.* **2002**, *14*, 5153.
- [39] M. H. Bartl, S. W. Boettcher, E. L. Hu, G. D. Stucky, *J. Am. Chem. Soc.* **2004**, *126*, 10826.
- [40] C. Ford, M. Singh, L. Lawson, J. B. He, V. John, Y. F. Lu, K. Papadopoulos, G. McPherson, A. Bose, *Colloids Surf. B* **2004**, *39*, 143.
- [41] S. Inagaki, S. Guan, T. Ohsuna, O. Terasaki, *Nature* **2002**, *416*, 304.
- [42] P. Kapoor Mahendra, Q. Yang, S. Inagaki, *J. Am. Chem. Soc.* **2002**, *124*, 15176.
- [43] K. Okamoto, M. P. Kapoor, S. Inagaki, *Chem. Commun.* **2005**, 1423.
- [44] P. Sierocki, H. Maas, P. Dragut, G. Richardt, F. Voegtle, L. De Cola, F. Brouwer, J. I. Zink, *J. Phys. Chem. B* **2006**, *110*, 24390.
- [45] M. A. Wahab, A. Sellinger, *Chem. Lett.* **2006**, 1240.
- [46] C. W. Lee, M. K. Oh, J. M. Jang, *Langmuir* **1993**, *9*, 1934.
- [47] L. Hammarstrom, M. Almgren, T. Norrby, *J. Phys. Chem.* **1992**, *96*, 5017.
- [48] M. Krieg, M. P. Pileni, A. M. Braun, M. Gratzel, *J. Colloid Interface Sci.* **1981**, *83*, 209.
- [49] T. Ban, D. Bruhwiler, G. Calzaferri, *J. Phys. Chem. B* **2004**, *108*, 16348.
- [50] T. D. Nguyen, H. R. Tseng, P. C. Celestre, A. H. Flood, Y. Liu, J. F. Stoddart, J. I. Zink, *Proc. Natl. Acad. Sci. USA* **2005**, *102*, 10029.
- [51] T. D. Nguyen, K. C. F. Leung, M. Liong, C. D. Pentecost, J. F. Stoddart, J. I. Zink, *Org. Lett.* **2006**, *8*, 3363.
- [52] K. C. F. Leung, T. D. Nguyen, J. F. Stoddart, J. I. Zink, *Chem. Mater.* **2006**, *18*, 5919.
- [53] T. D. Nguyen, Y. Liu, S. Saha, K. C.-F. Leung, J. F. Stoddart, J. I. Zink, *J. Am. Chem. Soc.* **2007**, *129*, 626.
- [54] K. Hoffmann, U. Resch-Genger, F. Marlow, *Microporous Mesoporous Mater.* **2000**, *41*, 99.
- [55] Z. H. Lei, A. Vaidyalingam, P. K. Dutta, *J. Phys. Chem. B* **1998**, *102*, 8557.
- [56] J. C. Scaiano, H. Garcia, *Acc. Chem. Res.* **1999**, *32*, 783.
- [57] K. B. Yoon, S. M. Hubig, J. K. Kochi, *J. Phys. Chem.* **1994**, *98*, 3865.
- [58] M. Borja, P. K. Dutta, *Nature* **1993**, *362*, 43.
- [59] T. Forster, *Discuss. Faraday Soc.* **1959**, *27*, 7.
- [60] E. Besson, A. Mehdi, D. A. Lerner, C. Reye, R. J. P. Corriu, *J. Mater. Chem.* **2005**, *15*, 803.
- [61] M. Alvaro, M. Benitez, D. Das, H. Garcia, E. Peris, *Chem. Mater.* **2005**, *17*, 4958.
- [62] N. Liu, D. R. Dunphy, P. Atanassov, S. D. Bunge, Z. Chen, G. P. Lopez, T. J. Boyle, C. J. Brinker, *Nano Lett.* **2004**, *4*, 551.
- [63] N. K. Mal, M. Fujiwara, Y. Tanaka, *Nature* **2003**, *421*, 350.
- [64] C. Y. Lai, B. G. Trewyn, D. M. Jeftinija, K. Jeftinija, S. Xu, S. Jeftinija, V. S. Y. Lin, *J. Am. Chem. Soc.* **2003**, *125*, 4451.
- [65] S. Angelos, E. Choi, F. Vogtle, L. De Cola, J. I. Zink, *J. Phys. Chem. C*, in press.
- [66] S. Saha, K. C. F. Leung, T. D. Nguyen, J. F. Stoddart, J. I. Zink, *Adv. Funct. Mater.* **2007**, *17*, 685.
- [67] S. Y. Chia, J. G. Cao, J. F. Stoddart, J. I. Zink, *Angew. Chem. Int. Ed.* **2001**, *40*, 2447.